UNIVERSITÉ LIBRE DE BRUXELLES
Faculté des Sciences
Département de Physique
Service d'Optique Nonlinéaire Théorique

Spontaneous Emission in a Solar Cell Geometry

Etienne Averlant

Promoteur :
Dr. Gregory Kozyreff

Mémoire présenté en vue de
l'obtention du grade de
master en Sciences Physiques

Année académique 2009 - 2010

Remerciements

Alors pour les remerciements collectifs, un tiercé dans le désordre alphabétique : Bendix, Billie, le C.K.C.B. et ses membres, Constance, Lionel, ma famille au complet, Mélanie, Orianne, Stéphanie, le service d'optique nonlinéaire théorique au complet. Aussi bien pour le soutien que les relectures ou même juste par envie.

Ensuite viennent tous ceux que j'ai oublié dans la liste ci-dessus : à tous ceux-là, je présente mes excuses.

Finalement, un merci sincère à Gregory Kozyreff, l'accueil qu'il m'a réservé dans le service, ses cours d'électrodynamique en cavité, de Mathematica et d'anglais, sa disponibilité. Sa patience surtout.

Summary

The role of photovoltaic(PV) cells is becoming more and more important in the production of renewable energies. However, this technology suffers from poor efficiency in converting solar energy into electrical current, especially because of the recombination of the excitons in the cell.

One can divide the exciton recombinations in two categories: the radiative and nonradiative recombinations. The aim of this work is to quantify how the radiative recombination of excitons depends on the cell geometrical and dielectric parameters.

To this end, we shall consider the solar cell as an electromagnetic cavity in which an exciton, modeled as an electrical dipole, experiences the electrical field of the cavity.

The dipole will be modeled as a two-level system whose wavefunction would be disturbed by the electrical field of vacuum fluctuations of the cavity. This will lead to an integral formula for the radiative recombination rate, which will be evaluated.

The results will also be simulated in Mathematica 7.0. Ways of improving solar cells will also be suggested.

Contents

Chapter 1

Introduction

1.1 Motivations

The total energy needs of the world keep getting higher[1]. Moreover, the greenhouse gases, as well as problems of treating the nuclear waste, tend to force thinking on alternative sources of energy. In the crowd of available solutions (wind energy, hydroelectric energy and many others), we decided to have a particular look on PV technology. This technology has taken advantage of the oil crisis in the 70's to begin being available to the general public. The technology also took advantage of the semiconductor industry as well as governmental development programs to finally become a very fast developping alternative source of energy[2]. The state of the art of the champions PV modules in converting solar energy into electrical energy is summed up in Fig. 1.1. One can then notice that the semiconductor PV cells have a great advance: when semiconductor PV cells reach a maximal 41.6% efficiency, the world champion "alternative technology" PV cell reaches only 11.1% efficiency. Although semiconductor PVs keep presenting higher efficiencies, care has to be given to alternative technologies, because of the difficulties to recycle semiconductor PV cells and the high extraction/manufacture cost inherent to semiconductors[3].

Thus, even if the efficiency of such alternative modules is far behind the semiconductor one, they require a special interest.

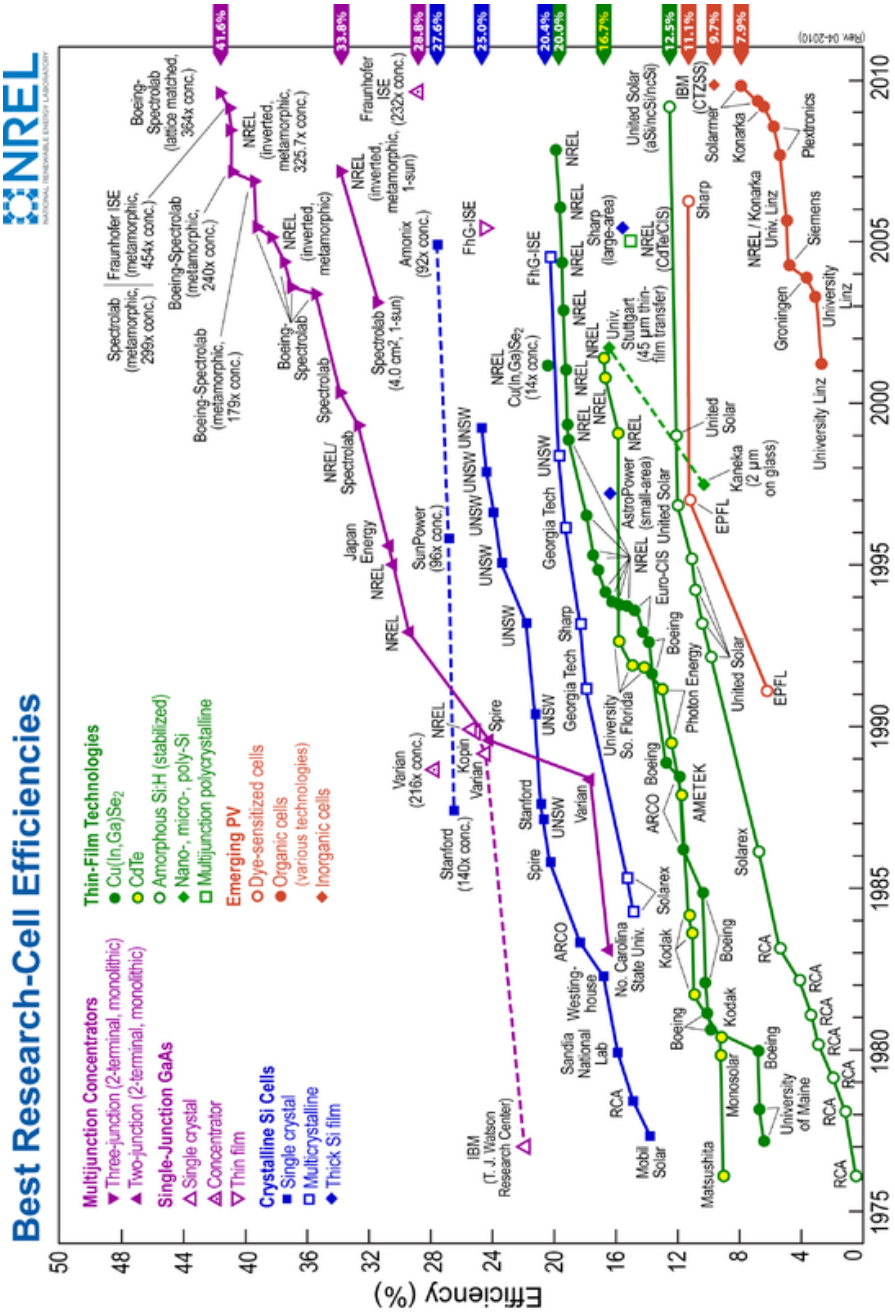

Figure 1.1: Efficiency of champion PV modules on converting solar energy into electricity. Source:[4]

1.2 Basics of solar cells

1.2.1 PN junction

In this section, we describe the basic phenomena responsible for the current emission by a PV cell. At first, we define the PN junction, to then proceed with the mechanism. Most atoms in the IV column of the periodic table form covalent crystals. As an example, the structure of a silicium crystal is depicted Fig 1.2.

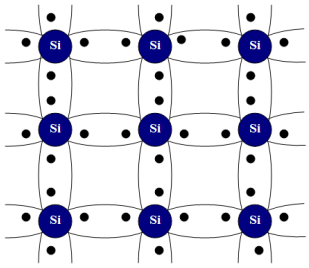

Figure 1.2: Scheme of a crystal of silicium. Source:[5]

This crystal can now be modified in order to have special properties, such as great conductivity of positive or negative charges. One would also talk of "doping". This doping mainly consists in injecting impurities (something else than the atoms normally present in the crystal) in a crystal, which would produce an excess of a type of carriers. One can then distinguish two types of doping: a semiconductor is said to be "n-doped" when it has a lack of positive charges, that is, an excess of negative charges. Such a crystal is more likely to conduct electrons than non doped silicium. It can be technologically realised by replacing a silicium atom by a pentavalent atom(e.g. phosphorus), as depicted in Fig. 1.3.

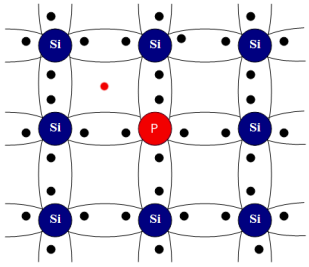

Figure 1.3: The Si atom in the middle has been replaced by a P atom. In red: the extra electron, free from bindings.

A semiconductor is also "p-doped" when it has an extra "hole", that is, when it has lost an electron. Instead of replacing a quadrivalent atom by a pentavalent atom as we did in the previous case, we here use a trivalent atom, e.g. boron. This is shown in Fig. 1.4.

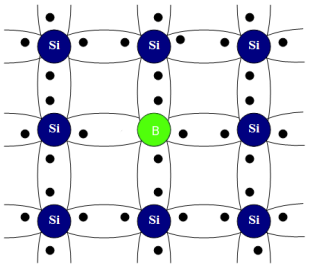

Figure 1.4: The Si atom in the middle has been replaced by a B atom. The hole diffuses in the crystal as a particle does; that is, this type of crystal is more likely to conduct holes

If the crystal is on one side p-doped and n-doped on the other, one would talk of a "pn-junction". In such arrangements, electrons from the donors atoms in the n-region recombine with positives holes from the acceptor atoms, producing a layer of negatively charged atoms[6]. This accumulation of charges creates an electrical field which changes the potential for the charge carriers, as depicted in Fig.1.5.

This electrical field is cucially important in a PV cell, as explained further on. An other important property of semiconductors is their characteristic energy levels. This work will not include a detailed theory of energy bands in semiconductors. Details can be found in reference [7]. Here, we will only use the result that the electronic energy structure of a pure semiconductor looks at a first approximation as depicted in Fig. 1.6.

One can then understand that for a photon to be absorbed by an electron in a semiconductor, it has to have an energy higher than the bandgap denoted in Figure 1.6. If this photon has enough energy, then it can be absorbed in the semiconductor material.

A PV cell is so built that light comes into the material from a n-doped region[8]. In the ideal case, this photon creates an electron-hole pair in the space charge region depicted in Fig.1.5. As this happens, an electron from the valence band is ejected and diffuses in the material, being subjected to the electrical field, to reach the top electrode. As the electron left the valence band, a place is there free. This free place, called "hole" locally attracts electrons from other bindings. Once a valence electron replaced the hole left by the conduction electron, everything is as if the hole diffused as a particle

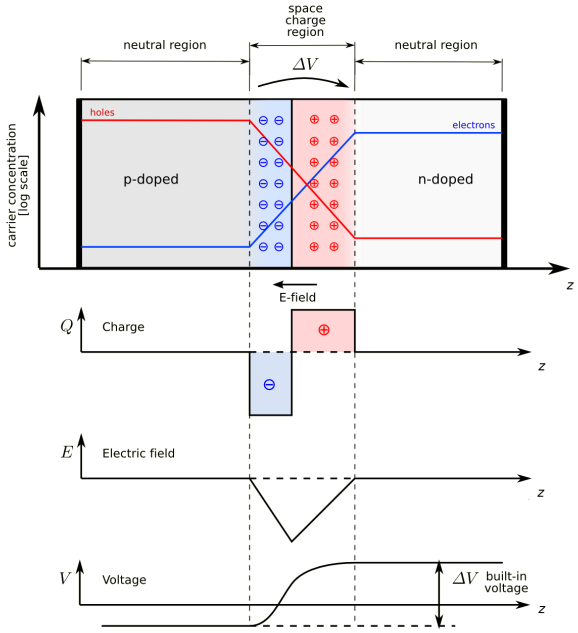

Figure 1.5: Charge, electrical potential and voltage in a PN junction. Source:[9]

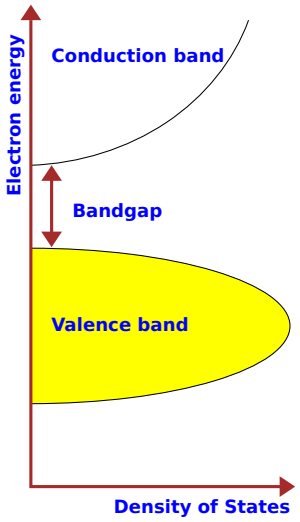

Figure 1.6: Typical energy band of electrons in a semiconductor: an electron in the valence band is bounded to its ion. In the conduction band, it behaves as a metallic electron. Source:[10]

would have diffused. The hole so diffuses down to the bottom electrode.

As an electron is on the top electrode and a hole on the bottom electrode, a direct current generation occurs. That is the mechanism of a PN-junction photovoltaic cell. One can then take a look on how high the created current is. To this end, one shall first consider the charge carrier population.

The charge carrier population n abides by the transport laws. By denoting the distance in the material to the light collecting surface of the device by z, the diffusion coefficient by D, the source term by G and the losses term by Γ, one has

$$D\frac{\partial^2 n}{\partial z^2} + G(z) - \Gamma n = 0. \tag{1.1}$$

Most photons do not create electron-hole pairs; actually, the photon flux as a function of the position in the cell $P(z)$ can be described by the Beer-Lambert law[8]:

$$P(z) = P(0)e^{-\alpha z}, \tag{1.2}$$

where α is the so called "absorbtion coefficient". This coefficient is a function of the photon energy, as well as of the considered material. We define the quantum efficiency of electron-hole pair generation Φ_1 such as

$$\Phi_1 = \frac{\text{Number of photons converted in charge carriers}}{\text{Number of photons absorbed in the material}} \tag{1.3}$$

The rate of creation of electron-hole pairs per unit volume thus yields

$$G(z) = -\Phi_1 \frac{dP(z)}{dz} = \alpha \Phi_1 P(0) e^{-\alpha z}. \tag{1.4}$$

Inserting this result in Eq. (1.1), one has

$$D\frac{d^2 n}{dz^2} + \alpha \Phi_1 P(0) e^{-\alpha z} - \Gamma n = 0. \tag{1.5}$$

We can therewith define the diffusion length L by

$$L = \sqrt{\frac{D}{\Gamma}}. \tag{1.6}$$

The solutions of Eq. (1.5) describe the transport of charge carriers. The current generation can also be computed. Further development can be found in [8].

1.2.2 Schottky barrier solar cell

The preceeding scheme is nowadays the most efficient one. Unfortunately, this architecture relies heavily on semiconductor technology: using this architecture with organic photoactive materials is a delicate issue. One of the problems one can encounter is the short diffusion length of the excitons, typically about a few nanometers [11]. Thus, even if the polymer PV cell has to be thick enough to absorb enough photons to create enough so called "excitons", it has to be thinner than a semiconductor system. The so called "Schottky architecture" is a special case of thin-film solar cells.

This section will describe the used polymer as a p-type material(as in [12]). Concerning the metal, a property has to be taken into account: the "ionization energy" of the metal. This property corresponds to the work needed to remove an electron from the metallic crystal. If this ionisation energy is low compared to that of the polymer (as depicted in Fig.1.7), then the metallic electrons will be more likely to populate the interface between the metal and the semiconductor, creating a potential characteristic of the so called "Schottky barrier". The metal-semiconductor interface is in this case depicted as a "rectifying contact". If the ionisation energy is close to the one of the polymer, a so called "nonrectifying contact" occurs: no electron passes through the interface. An electron energy diagram is depicted in Fig. 1.7.

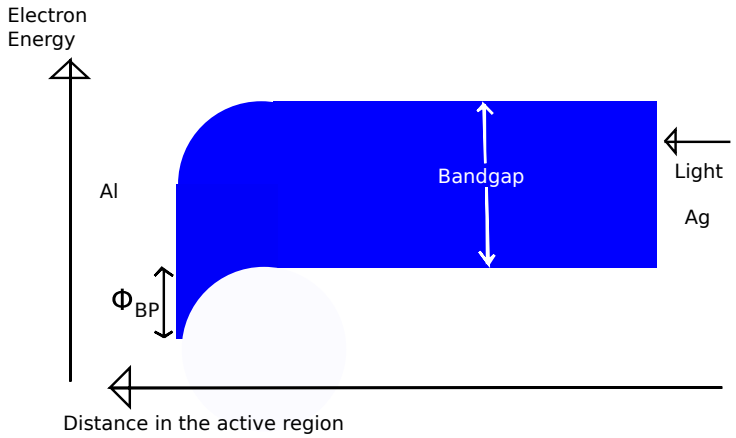

Figure 1.7: left: rectifying contact with Al, right: nonrectifying contact with Ag. Φ_{BP}: Schottky barrier.

A nonrectifying contact has no influence on the distribution of charges. Difference only occurs at the rectifying contact, where the charge distribution is similar to the one of a PN junction. As the energy distribution is similar, similar phenomena occur. In particular, Eq. (1.5) stills apply for the

excitons.

1.2.3 Schottky Polymer thin film PV

This architectrure applied to polymer thin film PV has special properties [12]: when a polymer absorbs a photon, it becomes an exciton (nothing more than an excited state of the polymer). This exciton diffuses to the space charge region at the rectifying interface between the metal and the polymer. Then a charge separation occurs and free charges diffuse in the material, once more because of the electrical field: electrons to the rectifying electrode, holes to the nonrectifying electrode. Excitons which recombine at the nonrectifying electrode produce no current: the free charge carriers are not subjected to a potential, and have therefore a negligible probability of producing current[12].

A potential difference then occurs between the electrodes, current generation is achieved.

1.3 Enhancing PV cells

Ways of improving solar cells are numerous: light trapping[13], multijunction [14], antireflexion coatings on the light collecting surface of the cell[15], oxide or insulator layer between the semiconductor metal interface[16]...

The study of polymer photovoltaics is particularly relevant([3],[17]), because of process costs and difficulties inherent to semiconductor PVs.

The polymer PVs also suffer from a short diffusion length of the excitons, resulting in a poor conversion efficiency.

We also define the quantum yield Φ_2 of a material as

$$\Phi_2 = \frac{\Gamma_{radiative}}{\Gamma}. \tag{1.7}$$

In the following sections, we will study the desexcitation of a material presenting a quantum yield close to unity. Such materials do not exist yet, but, if good results arise , one could consider looking for some.

1.4 Spontaneous emission in free space

In this section, we show how spontaneous emssion can be computed in free space. In the next chapter,the same approach will be applied to study spontaneous emission in a solar cell geometry. To this end, we consider a quantum

mechanical two-level system describing the exciton, and apply a time dependant perturbative treatment to quantify the interaction between this system and the vacuum electrical field.

1.4.1 Two-level system

We model the exciton as a two-level system. Physically speaking, the higher energy E_i state $|i\rangle$ corresponds to the existence of the exciton, whereas the lower energy E_f state $|f\rangle$ corresponds to the nonexistence of the exciton. At a time t, this exciton is represented by the wavefunction

$$|\psi\rangle = b_i(t)e^{-\frac{iE_it}{\hbar}}|i\rangle + b_f(t)e^{-\frac{iE_ft}{\hbar}}|f\rangle, \tag{1.8}$$

where, intitally

$$b_i(0) = 1, \qquad b_f(0) = 0. \tag{1.9}$$

The probability for the system to be in the state$|f\rangle$ is then the probability for the system to undergo a transition between states $|i\rangle$ and $|f\rangle$. One has thus

$$P_{i\to f}(t) = |b_f(t)|^2. \tag{1.10}$$

Given the electric field $\mathbf{E}$ and the electric moment $-e\mathbf{r}$ of the exciton, the interaction hamiltonian is [18]

$$H_i = -e\mathbf{E}\cdot\mathbf{r}. \tag{1.11}$$

We assume that this interaction hamiltonian has no diagonal coefficients. This Hamiltonian is a perturbation for the two-level system which induces a modification of the coefficients $b_i(t)$ and $b_f(t)$. We now let the electric field be a monochromatic wave, that is

$$\mathbf{E} = \mathbf{E_k}(\mathbf{x})e^{i\omega_k t}, \tag{1.12}$$

where the spatial dependence of the electrical field is contained in the vector $\mathbf{E_k}(\mathbf{x})$, further described as $\mathbf{E_k}$. The Schrödinger equation yields

$$i\hbar\frac{\partial|\psi\rangle}{\partial t} = H|\psi\rangle. \tag{1.13}$$

Projecting this equation on the eigenstate $\langle f|$, one has

$$i\hbar\frac{\partial}{\partial t}\left(b_fe^{-\frac{iE_ft}{\hbar}}\right) = b_fe^{-\frac{iE_ft}{\hbar}}E_f + \langle f|\mathbf{E_k}e^{i\omega_k t}\cdot(-e\mathbf{r})|(b_ie^{-\frac{iE_it}{\hbar}}|i\rangle + b_fe^{-\frac{iE_ft}{\hbar}}|f\rangle). \tag{1.14}$$

$$i\hbar\frac{\partial b_f}{\partial t}e^{-\frac{iE_f t}{\hbar}} = b_i e^{i\left(\omega_k t - \frac{E_i t}{\hbar}\right)}\langle f|\mathbf{E_k}\cdot(-e\mathbf{r})|i\rangle. \tag{1.15}$$

Expressing ω as

$$\omega = \frac{E_i - E_f}{\hbar}, \tag{1.16}$$

we get

$$\frac{\partial b_f}{\partial t} = -i\frac{b_i e^{i(\omega_k-\omega)t}\langle f|\mathbf{E_k}\cdot(-e\mathbf{r})|i\rangle}{\hbar}. \tag{1.17}$$

Moreover, as electromagnetic walengths are typically large in comparison of molecular dimensions, we define $\boldsymbol{\mu}$ such as

$$\langle f|\mathbf{E_k}\cdot(-e\mathbf{r})|i\rangle = \mathbf{E_k}\cdot\langle f|(-e\mathbf{r})|i\rangle = \mathbf{E_k}\cdot\boldsymbol{\mu}. \tag{1.18}$$

We thus have

$$\frac{\partial b_f}{\partial t} = -i\frac{b_i e^{i(\omega_k-\omega)t}\mathbf{E_k}\cdot\boldsymbol{\mu}}{\hbar}. \tag{1.19}$$

For short times, the coefficient $b_i(t)$ is approximately equal to its initial value, given by (1.9). We thus approximate Eq. (1.19) by

$$\frac{\partial b_f}{\partial t} = -i\frac{e^{i(\omega_k-\omega)t}\mathbf{E_k}\cdot\boldsymbol{\mu}}{\hbar}. \tag{1.20}$$

$$b_f = -\frac{\mathbf{E_k}\cdot\boldsymbol{\mu}}{\hbar}\left(\frac{e^{i(\omega_k-\omega)t}-1}{\omega_k-\omega}\right) \tag{1.21}$$

$$|b_f|^2 = \frac{|\mathbf{E_k}\cdot\boldsymbol{\mu}|^2}{(\omega_k-\omega)^2\hbar^2}\left|e^{i(\omega_k-\omega)t}-1\right|^2 \tag{1.22}$$

$$|b_f|^2 = \frac{|\mathbf{E_k}\cdot\boldsymbol{\mu}|^2}{(\omega_k-\omega)^2\hbar^2}\left|e^{\frac{i(\omega_k-\omega)t}{2}} - e^{\frac{-i(\omega_k-\omega)t}{2}}\right|^2 \tag{1.23}$$

$$P_{i\to f} = |b_f|^2 = \frac{4|\mathbf{E_k}\cdot\boldsymbol{\mu}|^2}{(\omega_k-\omega)^2\hbar^2}\sin^2\left[\frac{(\omega_k-\omega)t}{2}\right] \tag{1.24}$$

We introduce the angle ζ between $\boldsymbol{\mu}$ and $\mathbf{E_k}$ so that

$$P_{i\to f} = |b_f|^2 = \frac{4|\mathbf{E_k}|^2|\boldsymbol{\mu}|^2\cos^2(\zeta)}{(\omega_k-\omega)^2\hbar^2}\sin^2\left[\frac{(\omega_k-\omega)t}{2}\right] \tag{1.25}$$

We now consider an electrical field as a superposition of harmonic fields

$$\mathbf{E} = \sum_{\omega_k}\mathbf{E_k}e^{i\omega_k t}. \tag{1.26}$$

For a white spectrum presenting no phase corellation between its components, one has [19]:

$$\boxed{P_{i\to f} = \sum_{\omega_k} \frac{|\mathbf{E_k}|^2 |\boldsymbol{\mu}|^2 \cos^2(\zeta)}{\hbar^2} \frac{\sin^2[(\omega_k - \omega)t/2]}{(\omega_k - \omega)^2/4}.} \tag{1.27}$$

This treatment is expected to be valid for times large in regard of the atomic period, that is

$$\frac{1}{\omega_a} \ll t. \tag{1.28}$$

A typical value of $\frac{1}{\omega_a}$ (between the fondamental and the first excited state of an hydrogen atom) is

$$\frac{13.6\text{eV}}{\hbar} \approx 10^{-16}\text{s}, \tag{1.29}$$

which is neglectible in comparison with the other scales of time we will use.

But, as we supposed the system to vary low enough to suppose $b_i = 1$, time has to be small in comparison to a characteristic timescale of the system. Here, we take [19] the period of the Rabi oscillations into account:

$$t \ll \frac{\hbar}{|\boldsymbol{\mu} \cdot \mathbf{E_k}|}. \tag{1.30}$$

The Rabi oscillations occur at resonnance, when $\omega_k = \omega$. The system then oscillates between the states $|i\rangle$ and $|f\rangle$. After a period, the system is back to its initial state. The electrical field has now to be further described: as the medium in which the dipole evolves is vacuum, the dispersion relation between the pulsation and the wavenumber k yields, for the electric field as well as for the atomic frequency

$$\omega = ck_a, \qquad \omega_k = ck. \tag{1.31}$$

where

$$\mathbf{k} = \begin{pmatrix} k_x \\ k_y \\ k_z \end{pmatrix}, \qquad k = ||\mathbf{k}|| = \sqrt{k_x^2 + k_y^2 + k_z^2}. \tag{1.32}$$

In the limit of a large domain, the set of electromagnetic modes becomes dense, and (1.26) can be rewritten as

$$\mathbf{E} = \iiint_{\mathbb{R}^3_+} \mathbf{E_k} e^{i\omega_k t} \rho(\mathbf{k}) d\mathbf{k}, \tag{1.33}$$

where $\rho(\mathbf{k})$ is the density of electromagnetic modes presenting a wavevector $\mathbf{k}$. Eq. (1.27) then becomes

$$P_{i\to f} = \iiint_{\mathbb{R}^3_+} \frac{|\mathbf{E_k}|^2|\boldsymbol{\mu}|^2\cos^2(\zeta)}{\hbar^2}\frac{\sin^2[(\omega_k-\omega)t/2]}{(\omega_k-\omega)^2/4}\rho(\mathbf{k})d\mathbf{k}. \tag{1.34}$$

Using Eq. (1.31)

$$P_{i\to f} = \iiint_{\mathbb{R}^3_+} \frac{|\mathbf{E_k}|^2|\boldsymbol{\mu}|^2\cos^2(\zeta)}{\hbar^2}\frac{\sin^2[(k-k_a)ct/2]}{(k-k_a)^2c^2/4}\rho(\mathbf{k})d\mathbf{k} \tag{1.35}$$

Assuming a symmetry along the directions x and y, one has, with

$$k=\sqrt{k_\parallel^2+k_z^2}, \qquad k_\parallel\cos(\beta)=k_x, \qquad k_\parallel\sin(\beta)=k_y, \tag{1.36}$$

a density of states ρ independant of β. Thus,

$$P_{i\to f} = \iint_{\mathbb{R}^2_+} dk_z dk_\parallel \int_0^{\pi/2} d\beta \frac{|\mathbf{E_k}|^2|\boldsymbol{\mu}|^2\cos^2(\zeta)}{\hbar^2}\frac{\sin^2[(k-k_a)ct/2]}{(k-k_a)^2c^2/4} \times \rho(k_\parallel,k_z)k_\parallel dk_\parallel. \tag{1.37}$$

To perform the integration over $k_\parallel$, we use the following change of variable:

$$u=\frac{\left(\sqrt{k_z^2+k_\parallel^2}-k_a\right)ct}{2} \quad\rightarrow\quad \sqrt{k_z^2+k_\parallel^2}=k_a+\frac{2u}{ct}, \tag{1.38}$$

$$du=\frac{ct}{2}\frac{k_\parallel dk_\parallel}{\sqrt{k_z^2+k_\parallel^2}} \quad\rightarrow\quad k_\parallel dk_\parallel=\left(k_a+\frac{2u}{ct}\right)\frac{2du}{ct}. \tag{1.39}$$

Therewith,

$$P_{i\to f} = \int_0^\infty dk_z \int_0^{\pi/2} d\beta \int_{\frac{(k_z-k_a)ct}{2}}^\infty \frac{2|\mathbf{E_k}|^2|\boldsymbol{\mu}|^2\cos^2(\zeta)t}{c\hbar^2}\frac{\sin^2(u)}{u^2} \times \rho\left(\sqrt{\left(k_a+\frac{2u}{ct}\right)^2-k_z^2},k_z\right)\left(k_a+\frac{2u}{ct}\right)du. \tag{1.40}$$

We let now t tend to infinity,

$$P_{i\to f} = \frac{2\pi k_a t}{c\hbar^2}\int_0^{k_a} dk_z \int_0^{\frac{\pi}{2}} d\beta |\mathbf{E_k}|^2|\boldsymbol{\mu}|^2\cos^2(\zeta)\rho(k_\parallel,k_z). \tag{1.41}$$

The components of the electrical field presenting a frequency differing from the exciton frequency are not taken into account anymore. Physically, that means that, as t tends to infinity, only the resonnant contributions of the electromagnetic modes of the cavity have influence on the exciton. Thus, in the following, we do not make distinctions between (ω_k, k), respectingly pulsation and wavenumber of the electromagnetic field, and (ω, k_a), repectingly pulsation and wavenumber of the exciton. We now use (ω, k) to describe these quantities. Further assuming a symmetry on the (x, y) plane, one has

$$P_{i\to f} = \frac{\pi^2 kt}{c\hbar^2} \int_0^k dk_z |\mathbf{E_k}|^2 |\boldsymbol{\mu}|^2 \cos^2(\zeta) \rho(k_\parallel, k_z). \tag{1.42}$$

Or, equivalently:

$$\boxed{P_{i\to f} = \frac{\pi^2 \omega t \varepsilon_0 \mu_0}{\hbar^2} \int_0^k dk_z |\mathbf{E_k}|^2 |\boldsymbol{\mu}|^2 \cos^2(\zeta) \rho(k_\parallel, k_z)} \tag{1.43}$$

1.4.2 Mode density

In this section, we consider an empty cavity presenting an electromagnetic field. This cavity study let us compute a mode density inherent to the cavity. To derive the vacuum mode density, we will let the dimensions of the cavity tend to infinity. We thus consider, as depicted in Fig. 1.8, perfectly conducting walls in

$$x = 0, L_x \qquad y = 0, L_y \qquad z = 0, L_z \tag{1.44}$$

In this box, the wavevectors are quantified by the boundary conditions: indeed, the component of the electrical field in the plane of a perfectly conducting wall has to vanish on each perfectly conducting wall. We thus have

$$\mathbf{E_k} = \begin{bmatrix} E_x \cos(k_x x) \sin(k_y y) \sin(k_z z) \\ E_y \sin(k_x x) \cos(k_y y) \sin(k_z z) \\ E_z \sin(k_x x) \sin(k_y y) \cos(k_z z) \end{bmatrix}. \tag{1.45}$$

The Maxwell equation

$$\boldsymbol{\nabla} \cdot \mathbf{E} = 0, \tag{1.46}$$

further imposes that

$$\mathbf{E_k} \cdot \mathbf{k} = 0. \tag{1.47}$$

That means that, for each wavevector $\mathbf{k}$, the electric field has to be in the plane normal to this vector: there are two directions of polarisation for $\mathbf{E}$

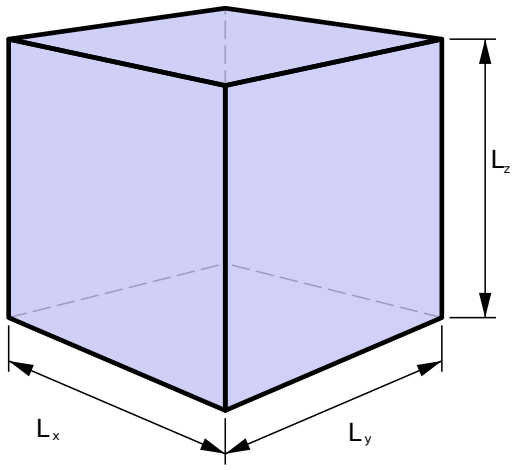

Figure 1.8: Electromagnetic cavity. Source: [20]

per wavevector $\mathbf{k}$. A factor 2 in the mode density has thus to be taken into account. Using Eq. (1.32), one has

$$k_x = \frac{m\pi}{L_x}, \tag{1.48}$$

$$k_y = \frac{n\pi}{L_y}, \tag{1.49}$$

$$k_z = \frac{p\pi}{L_z}, \tag{1.50}$$

where m, n and p are positive integers. The last set of equations also gives the distance between two adjacent modes in wavevector space

$$\triangle k_x = \frac{\pi}{L_x}, \tag{1.51}$$

$$\triangle k_y = \frac{\pi}{L_y}, \tag{1.52}$$

$$\triangle k_z = \frac{\pi}{L_z}. \tag{1.53}$$

The density of states is thus

$$\rho(k_x, k_y, k_z) = \frac{2}{\triangle k_x \triangle k_y \triangle k_z} = \frac{2L_xL_yL_z}{\pi^3} = \frac{2V}{\pi^3}. \tag{1.54}$$

Inserting this result in Eq. (1.43), one has

$$\boxed{P_{i\to f} = \frac{2V\omega\varepsilon_0\mu_0 t}{\pi\hbar^2}\int_0^k dk_z |\mathbf{E_k}|^2 |\boldsymbol{\mu}|^2 \cos^2(\zeta)} \tag{1.55}$$

1.4.3 Amplitude of the electrical field

In this section, we will choose the amplitude $|\mathbf{E_k}|^2$ to make it correspond to the electromagnetic energy of vacuum. The total electromagnetic energy of the system is

$$W = \iiint_V \left(\frac{\varepsilon_0 |\mathbf{E}|^2 + \mu_0 |\mathbf{H}|^2}{2} \right) d\mathbf{x}. \tag{1.56}$$

When the dimensions of the box tend to infinity, the system becomes isotropic: we thus choose the polarisation of the electrical field to be x, and its wavector to be directed in the direction $(\mathbf{e_y} + \mathbf{e_z})$

$$\begin{aligned} \mathbf{E_k} &= E_x \sin(k_y y) \sin(k_y z) \mathbf{e_x}, & (1.57) \\ |\mathbf{E}|^2 &= E_x^2 \sin^2(k_y y) \sin^2(k_y z). & (1.58) \end{aligned}$$

The Maxwell equations then give

$$\boldsymbol{\nabla} \times \mathbf{E_k} = i\mu_0 \omega \mathbf{H_k} \tag{1.59}$$

$$E_x \begin{bmatrix} 0 \\ k_y \sin(k_y y) \cos(k_y z) \\ -k_y \cos(k_y y) \sin(k_y z) \end{bmatrix} = i\mu_0 \omega \mathbf{H_k} \tag{1.60}$$

$$|\mathbf{H_k}|^2 = \frac{E_x^2 k_y^2}{\mu_0^2 \omega^2} \left[\sin^2(k_y y) \cos^2(k_y z) + \cos^2(k_y y) \sin^2(k_y z) \right]. \tag{1.61}$$

Taking a mean value for the terms oscillating with spatial coordinates,

$$\left\langle \frac{\varepsilon_0 |\mathbf{E_k}|^2 + \mu_0 |\mathbf{H_k}|^2}{2} \right\rangle_{\mathbf{x}} = \frac{\varepsilon_0 E_x^2}{4} \left\langle \sin^2(k_y y) + \sin^2(k_y z) \right\rangle_{\mathbf{x}}. \tag{1.62}$$

$$\left\langle \frac{\varepsilon_0 |\mathbf{E_k}|^2 + \mu_0 |\mathbf{H_k}|^2}{2} \right\rangle_{\mathbf{x}} = \frac{\varepsilon_0 E_x^2}{4}. \tag{1.63}$$

Thus, Eq. (1.56) gives

$$W = \frac{V \varepsilon_0 E_x^2}{4}, \tag{1.64}$$

We want this energy to be the one of the vacuum, that is ([21] p.184) $\hbar\omega/2$. Therewith, one gets

$$E_x^2 = \frac{2\hbar\omega}{\varepsilon_0 V} \tag{1.65}$$

We thus have, by taking a mean value for the spatial coordinates

$$|\mathbf{E_k}|^2 = \frac{E_x^2}{4} = \frac{\hbar\omega}{2\varepsilon_0 V} \tag{1.66}$$

Equation (1.55) thus becomes

$$P_{i\to f} = \frac{\omega^2 \mu_0 t}{\pi\hbar} \int_0^k dk_z |\boldsymbol{\mu}|^2 \cos^2(\zeta) \tag{1.67}$$

We now suppose a random orientation of $\boldsymbol{\mu}$: we thus take a mean value for $\cos^2(\zeta)$. As ζ is an angle between two vectors, the mean value of $\cos^2(\zeta)$ is $1/3$. Equation (1.67) then becomes

$$P_{i\to f} = \frac{\omega^2 \mu_0 t}{3\pi\hbar} \int_0^k dk_z |\boldsymbol{\mu}|^2 \tag{1.68}$$

$$P_{i\to f} = \frac{\omega^2 k \mu_0 |\boldsymbol{\mu}|^2 t}{3\pi\hbar} \tag{1.69}$$

$$P_{i\to f} = \frac{\omega^3 \sqrt{\varepsilon_0} \mu_0^{3/2} |\boldsymbol{\mu}|^2 t}{3\pi\hbar} \tag{1.70}$$

We then define the spontaneous desexcitation rate in vacuum Γ_0 such as

$$\Gamma_0 = \frac{P_{i\to f}}{t}. \tag{1.71}$$

$$\Gamma_0 = \frac{\omega^3 \sqrt{\varepsilon_0} \mu_0^{3/2} |\boldsymbol{\mu}|^2}{3\pi\hbar} \tag{1.72}$$

In a medium of permittivity ε_1, one has

$$\boxed{\Gamma_1 = \frac{\omega^3 \mu_0^{3/2} \sqrt{\varepsilon_1} |\boldsymbol{\mu}|^2}{3\pi\hbar}} \tag{1.73}$$

Chapter 2

Fermi Golden Rule in a solar cell geometry

The solar cell depicted in Fig. 2.1 is modelled as in Fig. 2.2. This cell is modelled as a cavity enclosed by perfect mirrors at

$$x = 0, L_x, \qquad y = 0, L_y, \qquad z = 0, h + d + L_z. \tag{2.1}$$

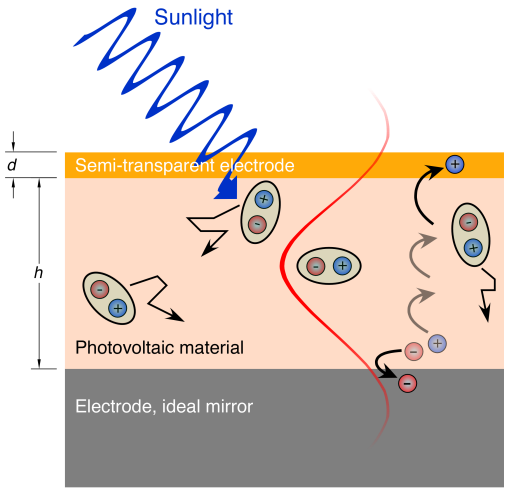

Figure 2.1: Scheme of the cell studied. Length of the semi transparent electrode: d. Length of the active region: h.Source:[11]

The region 1 is the active region where excitons are created. It is a polymer whose quantum efficiency is close to 1. The semitransparent electrode is

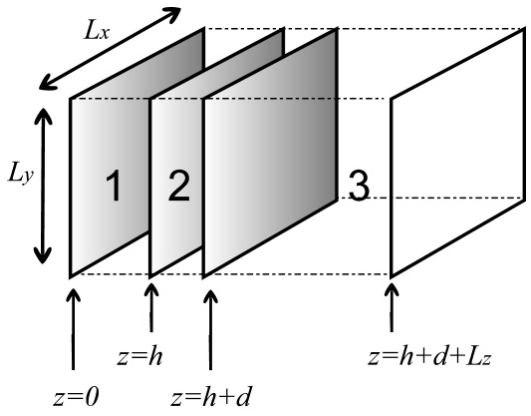

Figure 2.2: Geometry of the problem; region 1:active material, permittivity ε_1, region 2: semi transparent electrode, permittivity ε_2, region 3: air, permittivity ε_0.

a slice of transparent conductive oxide, such as indium tin oxide, fluorine tin oxide or zinc oxide [22]. We do not take into account the permeabilities of the media. The transverse dimensions are, in practice, about a couple of centimeters, while other dimensions are on a nanoscale range: the wavelengths are mainly in infrared and visible range of the electromagnetic spectrum, the diffusion length of the excitons is around [11] 5nm, the active region is approximatively 100nm thick, while the semitransparent electrode is about 5nm thick. We thus let the transverse dimensions tend to infinity.

In this chapter, we derive expressions for the mode density as well as for the spatial dependance of the electromagnetic field $\mathbf{E_k}$. The conclusion of this chapter will be an expression of the transition probability $P_{i\to f}$ as a function of the geometric and dielectric parameters of the PV cell.

The mode density derived in Eq. (1.54) is used in this chapter: as the volume of the third region is arbitrarly large, we do not take the first and second region in the development of this density of states.

As the medium is not homogeneous anymore, we introduce an alternative wavenumber, whose expression yields

$$q_i^2 + k_\parallel^2 = n_i^2 k^2, \tag{2.2}$$

where $n_i = \sqrt{\frac{\varepsilon_i}{\varepsilon_0}}$ stands for the refractive index of region i. In the third region, one has

$$q_3 = k_z. \tag{2.3}$$

2.1 Electromagnetic modes

The Maxwell equations [23] are

$$\boldsymbol{\nabla} \times \mathbf{H_k} = -i\omega\varepsilon \mathbf{E_k}, \qquad \boldsymbol{\nabla} \cdot \mathbf{H_k} = 0, \tag{2.4}$$

$$\boldsymbol{\nabla} \times \mathbf{E_k} = i\omega\mu \mathbf{H_k}, \qquad \boldsymbol{\nabla} \cdot \mathbf{E_k} = 0. \tag{2.5}$$

The geometry of the system invites to split $\mathbf{H_k}$ and $\mathbf{E_k}$ into

$$\mathbf{H_k} = H_z \mathbf{e_z} + \mathbf{H_t}, \qquad \mathbf{E} = E_z \mathbf{e_z} + \mathbf{E_t}, \qquad \boldsymbol{\nabla}_t = \begin{pmatrix} \frac{\partial}{\partial x} \\ \frac{\partial}{\partial y} \\ 0 \end{pmatrix}, \tag{2.6}$$

where the subscript t refers to transverse components. Eqs. (2.4) and (2.5) become

$$\frac{\partial}{\partial z}(\mathbf{e_z} \times \mathbf{H_t}) + \boldsymbol{\nabla}_t \times H_z \mathbf{e_z} + \boldsymbol{\nabla}_t \times \mathbf{H_t} = -i\omega\varepsilon \mathbf{E}, \tag{2.7}$$

$$\frac{\partial}{\partial z}(\mathbf{e_z} \times \mathbf{E_t}) + \boldsymbol{\nabla}_t \times E_z \mathbf{e_z} + \boldsymbol{\nabla}_t \times \mathbf{E_t} = i\omega\mu \mathbf{H}. \tag{2.8}$$

The electromagnetics modes can be split in two categories:

1. Transverse electric (TE) in the z direction if the component of the electric field in this direction is zero

2. Transverse magnetic (TM) in the z direction if the component of the magnetic field in this direction is zero

2.1.1 Transverse electric modes

In this section, we compute the desexcitation rate induced by transverse electric modes. To this end, we use continuity equations, expliciting the structure of the TE modes, before normalising the amplitude to make the energy of those modes equal to the vacuum electromagnetic energy.

Continuity and characteristic equations

In this section, we make use of the Maxwell equations in the case of the TE modes to derive the spatial dependence of the electric field. To this end, we set the continuity equations of the system. One has, for those modes, as e.g. in[23],

$$H_z = \psi, \tag{2.9}$$

$$\mathbf{H_t} = \frac{\partial}{k_\parallel^2 \partial z}\begin{pmatrix} \frac{\partial H_z}{\partial x} \\ \frac{\partial H_z}{\partial y} \end{pmatrix}, \qquad \mathbf{E_t} = \frac{i\mu\omega}{k_\parallel^2}\begin{pmatrix} \frac{\partial H_z}{\partial y} \\ -\frac{\partial H_z}{\partial x} \end{pmatrix}. \tag{2.10}$$

In $z = 0$ and $z = L_z + h + d$ stand perfect mirrors: H_z has then to vanish for those conditions. On the transverse walls, the component of the electric field transverse to the surface has to do so; ψ has then the following form.

$$\psi_1 = S_1 \sin(q_1 z)\cos(k_x x)\cos(k_y y), \tag{2.11}$$
$$\psi_2 = (U_2 e^{iq_2(z-h)} + D_2 e^{-iq_2(z-h)})\cos(k_x x)\cos(k_y y), \tag{2.12}$$
$$\psi_3 = U_3(e^{iq_3(z-h-d)} - e^{2iq_3 L_z} e^{-iq_3(z-h-d)})\cos(k_x x)\cos(k_y y). \tag{2.13}$$

The transverse components of each field have to be continous at each interface between two regions. Thus, for the electrical field to have continuous components in the transverse directions, the function ψ has to satisfy

$$[\psi]_-^+ = 0 \tag{2.14}$$

at each interface. For the transverse components of the magnetic field, that is

$$\left[\frac{\partial \psi}{\partial z}\right]_-^+ = 0 \tag{2.15}$$

at each interface. We now develop those transition conditions between the second and the third region.

$$U_2 e^{iq_2 d} + D_2 e^{-iq_2 d} = U_3(1 - e^{2iq_3 L_z}) \tag{2.16}$$
$$q_2(U_2 e^{iq_2 d} - D_2 e^{-iq_2 d}) = q_3 U_3(1 + e^{2iq_3 L_z}) \tag{2.17}$$

Excluding the $e^{2iq_3 L_z}$ term, one gets

$$(q_3 + q_2)U_2 e^{iq_2 d} + (q_3 - q_2)D_2 e^{-iq_2 d} = 2q_3 U_3 \tag{2.18}$$

which can be rewritten as

$$U_2 e^{iq_2 d} + \frac{q_3 - q_2}{q_3 + q_2} D_2 e^{-iq_2 d} = 2\frac{q_3}{q_3 + q_2} U_3 \tag{2.19}$$

We now define the reflexion coefficients as

$$R_{12} = \frac{q_1 - q_2}{q_1 + q_2}, \qquad R_{23} = \frac{q_2 - q_3}{q_2 + q_3}. \tag{2.20}$$

So that

$$e^{2iq_2 d} U_2 - R_{23} D_2 = (1 - R_{23}) e^{iq_2 d} U_3 \tag{2.21}$$

We now consider the transition conditions between regions 1 and 2

$$\begin{aligned} S_1 \sin(q_1 h) &= U_2 + D_2 && (2.22)\\ q_1 S_1 \cos(q_1 h) &= i q_2 (U_2 - D_2) && (2.23) \end{aligned}$$

Excluding S_1, it comes

$$i q_2 \sin(q_1 h)(U_2 - D_2) = q_1 \cos(q_1 h)(U_2 + D_2), \tag{2.24}$$

which can be rewritten as

$$\left[q_1 \cos(q_1 h) - i q_2 \sin(q_1 h)\right] U_2 + \left[q_1 \cos(q_1 h) + i q_2 \sin(q_1 h)\right] D_2 = 0 \tag{2.25}$$

After some algebra, one has

$$\left(\frac{q_1 - q_2}{q_1 + q_2} e^{2 i q_1 h} + 1\right) U_2 + \left(e^{2 i q_1 h} + \frac{q_1 - q_2}{q_1 + q_2}\right) D_2 = 0. \tag{2.26}$$

Inserting Eq. (2.20) in Eq. (2.26), it comes

$$\left(R_{12} e^{2 i q_1 h} + 1\right) U_2 + \left(e^{2 i q_1 h} + R_{12}\right) D_2 = 0. \tag{2.27}$$

Eqs.(2.21) and (2.27) can be rewritten as

$$\begin{pmatrix} e^{2 i q_2 d} & -R_{23} \\ R_{12} e^{2 i q_1 h} + 1 & e^{2 i q_1 h} + R_{12} \end{pmatrix} \begin{pmatrix} U_2 \\ D_2 \end{pmatrix} = \begin{pmatrix} (1 - R_{23}) e^{i q_2 d} U_3 \\ 0 \end{pmatrix}. \tag{2.28}$$

We then define Δ as

$$\begin{aligned} \Delta &= \begin{vmatrix} e^{2 i q_2 d} & -R_{23} \\ R_{12} e^{2 i q_1 h} + 1 & e^{2 i q_1 h} + R_{12} \end{vmatrix}, && (2.29)\\ \Delta &= e^{2 i (q_1 h + q_2 d)} + R_{12}(e^{2 i q_2 d} + R_{23} e^{2 i q_1 h}) + R_{23}. && (2.30) \end{aligned}$$

U_2 and D_2 thus yield

$$\begin{aligned} U_2 &= \frac{(1 - R_{23}) e^{i q_2 d} U_3 (e^{2 i q_1 h} + R_{12})}{\Delta}, && (2.31)\\ D_2 &= -\frac{(1 - R_{23}) e^{i q_2 d} U_3 (e^{2 i q_1 h} R_{12} + 1)}{\Delta}. && (2.32) \end{aligned}$$

Knowing U_2 and D_2, we can use Eq. (2.22):

$$S_1 \frac{e^{i q_1 h} - e^{-i q_1 h}}{2 i} = \frac{(1 - R_{23}) e^{i q_2 d} U_3}{\Delta} \left[e^{2 i q_1 h} + R_{12} - (e^{2 i q_1 h} R_{12} + 1)\right], \tag{2.33}$$

after some calculations, it comes

$$\boxed{S_1 = \frac{2i(1-R_{23})(1-R_{12})e^{i(q_1h+q_2d)}U_3}{\Delta}} \tag{2.34}$$

Injecting the equations (2.31) and (2.32) in Eq. (2.16), one has

$$\frac{(1-R_{23})e^{iq_2d}U_3(e^{2iq_1h}+R_{12})}{\Delta}e^{iq_2d} - \frac{(1-R_{23})e^{iq_2d}U_3(e^{2iq_1h}R_{12}+1)}{\Delta}e^{-iq_2d} = U_3(1-e^{2iq_3L_z}) \tag{2.35}$$

Finally, using Eq. (2.30),

$$\boxed{\Delta e^{2iq_3L_z} = R_{23}e^{2i(q_1h+q_2d)} + R_{23}R_{12}e^{2iq_2d} + e^{2iq_1h}R_{12} + 1} \tag{2.36}$$

This is the characteristic equation of the system. A completely equivalent expression, using trigonometric functions yields

$$\tan(q_1h)\tan(q_2d)\tan(q_3L_z) - \frac{q_1\tan(q_3L_z)}{q_2} - \frac{q_3\tan(q_1h)}{q_2} = \frac{q_1q_3\tan(q_2d)}{q_2^2} \tag{2.37}$$

A discussion about its properties will take place in chapter 4.

Normalisation

In this section, we normalise the amplitude of the electromagnetic modes so that their energy will be the one the vacuum. To this end, we derive an expression for the TE modes in the third region, making the assumption that all the energy is in. We now normalise U_3, taking the total energy of the system into account. We have:

$$\mathbf{E_k} = \frac{i\mu_0\omega}{k_\parallel^2}\begin{pmatrix} \frac{\partial\psi_i}{\partial y} \\ -\frac{\partial\psi_i}{\partial x} \\ 0 \end{pmatrix} \qquad \mathbf{H_k} = \begin{pmatrix} \frac{\partial^2\psi_i}{k_\parallel^2\partial z\partial x} \\ \frac{\partial^2\psi_i}{k_\parallel^2\partial z\partial y} \\ \psi_i \end{pmatrix} \tag{2.38}$$

where $i \in \{1,2,3\}$ is the number of the region in which the field is being expressed. The total electromagnetic energy of the system is:

$$W = \int_0^{L_x} dx \int_0^{L_y} dy \int_0^{L_z} dz \left(\frac{\varepsilon|\mathbf{E}|^2 + \mu_0|\mathbf{H}|^2}{2}\right) \tag{2.39}$$

As the region 3 is arbitrarly large, we consider that all the energy is in:

$$W = \int_0^{L_x} dx \int_0^{L_y} dy \int_{h+d}^{L_z} dz \left(\frac{\varepsilon_0 |\mathbf{E}|^2 + \mu_0 |\mathbf{H}|^2}{2} \right) \tag{2.40}$$

We now have to calculate the electrical field in the third region. First, we inject Eq. (2.13) in (2.38)

$$\mathbf{E_k} = \frac{i\mu_0 \omega U_3 (e^{iq_3(z-h-d)} - e^{2iq_3 L_z} e^{-iq_3(z-h-d)})}{k_\parallel^2} \begin{pmatrix} -k_y \cos(k_x x) \sin(k_y y) \\ k_x \sin(k_x x) \cos(k_y y) \\ 0 \end{pmatrix}. \tag{2.41}$$

It comes

$$\varepsilon_0 |\mathbf{E}|^2 = \frac{\varepsilon_0 \mu_0^2 \omega^2 |U_3|^2 |e^{iq_3(z-h-d)} - e^{2iq_3 L_z} e^{-iq_3(z-h-d)}|^2}{k_\parallel^4} \Big[k_y^2 \cos^2(k_x x) \sin^2(k_y y) + k_x^2 \sin^2(k_x x) \cos^2(k_y y) \Big] \tag{2.42}$$

We now derive an expression for $|\mathbf{H}|^2$ in the third region, using the same method:

$$\mathbf{H_k} = \begin{pmatrix} \frac{-iq_3 k_x U_3 (e^{iq_3(z-h-d)} + e^{2iq_3 L_z} e^{-iq_3(z-h-d)}) \sin(k_x x) \cos(k_y y)}{k_\parallel^2} \\ \frac{-iq_3 k_y U_3 (e^{iq_3(z-h-d)} + e^{2iq_3 L_z} e^{-iq_3(z-h-d)}) \cos(k_x x) \sin(k_y y)}{k_\parallel^2} \\ U_3 (e^{iq_3(z-h-d)} - e^{2iq_3 L_z} e^{-iq_3(z-h-d)}) \cos(k_x x) \cos(k_y y) \end{pmatrix} \tag{2.43}$$

It comes

$$\frac{|\mathbf{H}|^2}{|U_3|^2} = \frac{q_3^2 |e^{iq_3(z-h-d)} + e^{2iq_3 L_z} e^{-iq_3(z-h-d)}|^2}{k_\parallel^4} \Big[k_x^2 \sin^2(k_x x) \cos^2(k_y y) + k_y^2 \cos^2(k_x x) \sin^2(k_y y) \Big] + |e^{iq_3(z-h-d)} - e^{2iq_3 L_z} e^{-iq_3(z-h-d)}|^2 \cos^2(k_x x) \cos^2(k_y y). \tag{2.44}$$

Taking a mean value for the terms oscillating with spatial coordinates, one gets

$$\left\langle \frac{\varepsilon_0 |\mathbf{E}|^2 + \mu_0 |\mathbf{H}|^2}{2} \right\rangle_{\mathbf{x}} = \frac{|U_3|^2 \mu_0}{4} \left[\frac{2\varepsilon_0 \mu_0 \omega^2}{k_\parallel^4} \left(\frac{k_y^2 + k_x^2}{2} \right) + \frac{2q_3^2}{k_\parallel^4} \left(\frac{k_x^2 + k_y^2}{2} \right) + 1 \right] \tag{2.45}$$

It comes

$$\left\langle \frac{\varepsilon_0 |\mathbf{E}|^2 + \mu_0 |\mathbf{H}|^2}{2} \right\rangle_{\mathbf{x}} = \frac{|U_3|^2 \varepsilon_0 \mu_0^2 \omega^2}{2k_\parallel^2} \tag{2.46}$$

We then have

$$W = \frac{|U_3|^2 \varepsilon_0 \mu_0^2 \omega^2 V}{2k_\parallel^2} \tag{2.47}$$

Where V is the volume of the region 3. We want this energy to be equal to the energy of the vacuum $\frac{\hbar\omega}{2}$. This gives us

$$\boxed{|U_3|^2 = \frac{\hbar k_\parallel^2}{V \varepsilon_0 \mu_0^2 \omega}} \tag{2.48}$$

Transition probability induced by the TE modes

We are now in position to compute the transition probability induced by the TE modes. To this end, we compute $|\boldsymbol{\mu} \cdot \mathbf{E_k}|^2$ in the first region, before using Eq. (1.55). We thus have assumed that the density of modes is identical as the one of the vacuum case.

First, we compute the electrical field in the first region, using Eq. (2.38)

$$\mathbf{E_k} = \frac{S_1 i \mu_0 \omega \sin(q_1 z)}{k_\parallel^2} \begin{pmatrix} -k_y \sin(k_x x)\cos(k_y y) \\ k_x \cos(k_x x)\sin(k_y y) \\ 0 \end{pmatrix} \tag{2.49}$$

Inserting (2.34), it comes

$$\mathbf{E_k} = \frac{-2(1-R_{23})(1-R_{12}) e^{i(q_1 h + q_2 d)} U_3 \mu_0 \omega \sin(q_1 z)}{\Delta k_\parallel^2} \begin{pmatrix} -k_y \sin(k_x x)\cos(k_y y) \\ k_x \cos(k_x x)\sin(k_y y) \\ 0 \end{pmatrix} \tag{2.50}$$

We now take as convention for the orientation of $\boldsymbol{\mu}$

$$\boldsymbol{\mu} = |\boldsymbol{\mu}| \begin{pmatrix} \sin(\Psi)\cos(\phi) \\ \sin(\Psi)\sin(\phi) \\ \cos(\Psi) \end{pmatrix} \tag{2.51}$$

where ϕ and Ψ are Euler angles. We then have:

$$|\mathbf{E} \cdot \boldsymbol{\mu}|^2 = \frac{4|\boldsymbol{\mu}|^2 |1-R_{12}|^2 |1-R_{23}|^2 \sin^2(q_1 z) \mu_0^2 \omega^2 |U_3|^2 \sin^2(\Psi)}{|\Delta|^2 k_\parallel^4}$$
$$\times (k_y^2 \cos^2(\phi)\sin^2(k_x x)\cos^2(k_y y) + k_x^2 \sin^2(\phi)\cos^2(k_x x)\sin^2(k_y y)). \tag{2.52}$$

Inserting Eq. (2.48),

$$|\mathbf{E} \cdot \boldsymbol{\mu}|^2 = \frac{4|\boldsymbol{\mu}|^2 |1-R_{12}|^2 |1-R_{23}|^2 \sin^2(q_1 z) \omega \hbar \sin^2(\Psi)}{|\Delta|^2 k_\parallel^2 V \varepsilon_0}$$
$$\times \left[k_y^2 \cos^2(\phi)\sin^2(k_x x)\cos^2(k_y y) + k_x^2 \sin^2(\phi)\cos^2(k_x x)\sin^2(k_y y)\right]. \tag{2.53}$$

We now take an average value on x and y, as well as on ϕ

$$\langle|\mathbf{E}\cdot\boldsymbol{\mu}|^2\rangle_{x,y,\phi} = \frac{|\boldsymbol{\mu}|^2|1-R_{12}|^2|1-R_{23}|^2\sin^2(q_1 z)\omega\hbar\sin^2(\Psi)}{2|\Delta|^2 V\varepsilon_0} \tag{2.54}$$

Finally, using the desexcitation rule (1.55), one has:

$$\boxed{P^{TE}_{i\to f} = \frac{\sin^2(\Psi)|\boldsymbol{\mu}|^2\omega^2\mu_0 t}{2\pi\hbar}\int_0^k dk_z \frac{|1-R_{12}|^2|1-R_{23}|^2\sin^2(q_1 z)}{|\Delta|^2}} \tag{2.55}$$

2.1.2 Transverse magnetic modes

In this section, we compute the desexcitation rate induced by transverse magnetic modes. To this end, we use continuity equations, expliciting the structure of the TM modes, before normalising the amplitude to make the energy of those modes equal to the vacuum electromagnetic energy.

Continuity and characteristic equations

In this section, we use Maxwell equations in the case of the TM modes to derive the spatial dependence of the electric field. To this end, we set the continuity equations of the system. One has, for those modes, as e.g. in[23],

$$E_z = \psi, \tag{2.56}$$

$$\mathbf{E_t} = \frac{\partial}{k_\parallel^2\partial z}\begin{pmatrix}\frac{\partial E_z}{\partial x}\\ \frac{\partial E_z}{\partial y}\end{pmatrix}, \qquad \mathbf{H_t} = \frac{-i\varepsilon\omega}{k_\parallel^2}\begin{pmatrix}\frac{\partial E_z}{\partial y}\\ -\frac{\partial E_z}{\partial x}\end{pmatrix}. \tag{2.57}$$

In $z=0$ and $z = L_z + h + d$ stand perfect mirrors: $\mathbf{E_t}$ has to vanish for those conditions. On the transverse walls, E_z has to do so; ψ has thus the following form

$$\psi_1 = C_1\cos(q_1 z)\sin(k_x x)\sin(k_y y) \tag{2.58}$$
$$\psi_2 = (U_2 e^{iq_2(z-h)} + D_2, e^{-iq_2(z-h)})\sin(k_x x)\sin(k_y y) \tag{2.59}$$
$$\psi_3 = U_3(e^{iq_3(z-h-d)} + e^{2iq_3 L_z}, e^{-iq_3(z-h-d)})\sin(k_x x)\sin(k_y y). \tag{2.60}$$

The transverse components of each field have to be continuous at each interface between two media. Thus, for the electrical field to have continuous components in the transverse directions, thefunction ψ has to satisfy

$$\left[\frac{\partial\psi}{\partial z}\right]_-^+ = 0 \tag{2.61}$$

at each interface. For the transverse components of the magnetical field, this yields

$$[\varepsilon\psi]_-^+ = 0. \tag{2.62}$$

We now develop those transition conditions between the second and the third region

$$\varepsilon_2(U_2 e^{iq_2 d} + D_2 e^{-iq_2 d}) = \varepsilon_0 U_3(1 + e^{2iq_3 L_z}) \tag{2.63}$$
$$iq_2(U_2 e^{iq_2 d} - D_2 e^{-iq_2 d}) = iq_3 U_3(1 - e^{2iq_3 L_z}) \tag{2.64}$$

Excluding the $e^{2iq_3 L_z}$ term, one gets

$$U_2 e^{iq_2 d} + \frac{\varepsilon_2 q_3 - \varepsilon_0 q_2}{\varepsilon_2 q_3 + \varepsilon_0 q_2} D_2 e^{-iq_2 d}) = 2\frac{\varepsilon_0 q_3}{\varepsilon_2 q_3 + \varepsilon_0 q_2} U_3 \tag{2.65}$$

We now define the reflexion coefficients as

$$r_{12} = \frac{\varepsilon_2 q_1 - \varepsilon_1 q_2}{\varepsilon_2 q_1 + \varepsilon_1 q_2}, \qquad r_{23} = \frac{\varepsilon_0 q_2 - \varepsilon_2 q_3}{\varepsilon_0 q_2 + \varepsilon_2 q_3}, \tag{2.66}$$

So that

$$e^{2iq_2 d} U_2 - r_{23} D_2 = \frac{\varepsilon_0(1 - r_{23}) e^{iq_2 d} U_3}{\varepsilon_2} \tag{2.67}$$

We now consider the transition conditions between regions 1 and 2

$$\varepsilon_1 C_1 \cos(q_1 h) = \varepsilon_2(U_2 + D_2) \tag{2.68}$$
$$-q_1 C_1 \sin(q_1 h) = iq_2(U_2 - D_2) \tag{2.69}$$

Excluding C_1, it comes

$$q_1 \sin(q_1 h)\varepsilon_2(U_2 + D_2) + i\varepsilon_1 \cos(q_1 h) q_2(U_2 - D_2) = 0 \tag{2.70}$$

Afeter some algebra,

$$\left(\frac{\varepsilon_2 q_1 - \varepsilon_1 q_2}{\varepsilon_2 q_1 + \varepsilon_1 q_2} e^{2iq_1 h} - 1\right) U_2 + \left(e^{2iq_1 h} - \frac{\varepsilon_2 q_1 - \varepsilon_1 q_2}{\varepsilon_2 q_1 + \varepsilon_1 q_2}\right) D_2 = 0 \tag{2.71}$$

Inserting (2.66) in (2.71), it comes

$$\left(r_{12} e^{2iq_1 h} - 1\right) U_2 + \left(e^{2iq_1 h} - r_{12}\right) D_2 = 0 \tag{2.72}$$

Eqs. (2.67) and (2.72) can be rewritten as

$$\begin{pmatrix} e^{2iq_2 d} & -r_{23} \\ r_{12} e^{2iq_1 h} - 1 & e^{2iq_1 h} - r_{12} \end{pmatrix} \begin{pmatrix} U_2 \\ D_2 \end{pmatrix} = \begin{pmatrix} \frac{\varepsilon_0(1 - r_{23}) e^{iq_2 d} U_3}{\varepsilon_2} \\ 0 \end{pmatrix} \tag{2.73}$$

We then define δ as

$$\delta = \begin{vmatrix} e^{2iq_2d} & -r_{23} \\ r_{12}e^{2iq_1h} - 1 & e^{2iq_1h} - r_{12} \end{vmatrix} \tag{2.74}$$

$$\delta = e^{2i(q_1h+q_2d)} + r_{12}(r_{23}e^{2iq_1h} - e^{2iq_2d}) - r_{23} \tag{2.75}$$

U_2 and D_2 thus yield

$$U_2 = \frac{\varepsilon_0(1-r_{23})e^{iq_2d}U_3(e^{2iq_1h} - r_{12})}{\varepsilon_2\delta} \tag{2.76}$$

$$D_2 = -\frac{\varepsilon_0(1-r_{23})e^{iq_2d}U_3(r_{12}e^{2iq_1h} - 1)}{\varepsilon_2\delta} \tag{2.77}$$

Knowing U_2 and D_2, we can use Eq. (2.68):

$$\varepsilon_1 C_1 \cos(q_1h) = \frac{\varepsilon_0(1-r_{23})e^{iq_2d}U_3}{\delta}\left[e^{2iq_1h} - r_{12} - (r_{12}e^{2iq_1h} - 1)\right] \tag{2.78}$$

After some calculations, it comes

$$\boxed{C_1 = \frac{2\varepsilon_0(1-r_{23})e^{i(q_1h+q_2d)}(1-r_{12})U_3}{\varepsilon_1\delta}} \tag{2.79}$$

Injecting the equations (2.76) and (2.77) in (2.63), one has

$$\frac{(1-r_{23})e^{iq_2d}U_3(e^{2iq_1h} - r_{12})}{\delta}e^{iq_2d} - \frac{(1-r_{23})e^{iq_2d}U_3(r_{12}e^{2iq_1h} - 1)}{\delta}e^{-iq_2d} = U_3(1 + e^{2iq_3L_z}) \tag{2.80}$$

Finally, using Eq. (2.75)

$$\boxed{\delta e^{2iq_3L_z} = -r_{23}e^{2i(q_1h+q_2d)} + r_{12}r_{23}e^{2iq_2d} - r_{12}e^{2iq_1h} + 1} \tag{2.81}$$

This is the characteristic equation for the TM modes. A completely equivalent expression, using trigonometric functions yields

$$\tan(q_1h)\tan(q_2d)\tan(q_3L_z) = \frac{q_2}{\varepsilon_2}\left(\frac{\varepsilon_0\varepsilon_1 q_2\tan(q_2d)}{\varepsilon_2 q_1 q_3} + \frac{\varepsilon_0\tan(q_1h)}{q_3} + \frac{\varepsilon_1\tan(q_3L_z)}{q_1}\right) \tag{2.82}$$

A discussion about its properties will take place in chapter 4.

Normalisation

In this section, we normalise the amplitude of the electromagnetic modes so that their energy will be the one of the vacuum. To this end, we derive an expression for the TM modes in the third region, making the assumption that all the energy is in. We now normalise U_3, taking the total energy of the system into account. We have:

$$\mathbf{E_k} = \begin{pmatrix} \frac{\partial^2 \psi_i}{k_\parallel^2 \partial x \partial z} \\ \frac{\partial^2 \psi_i}{k_\parallel \partial y \partial z} \\ \psi_i \end{pmatrix} \qquad \mathbf{H_k} = \frac{\varepsilon_i \omega}{i k_\parallel^2} \begin{pmatrix} \frac{\partial \psi_i}{\partial y} \\ -\frac{\partial \psi_i}{\partial x} \\ 0 \end{pmatrix} \tag{2.83}$$

where $i \in \{1, 2, 3\}$ is the number of the region in which the field is being expressed. The total electromagnetic energy of the system is:

$$W = \int_0^{L_x} dx \int_0^{L_y} dy \int_0^{L_z} dz \left(\frac{\varepsilon |E|^2 + \mu_0 |H|^2}{2} \right) \tag{2.84}$$

As the region 3 is arbitrarly large, we consider that all the energy is in:

$$W = \int_0^{L_x} dx \int_0^{L_y} dy \int_{h+d}^{L_z} dz \left(\frac{\varepsilon_0 |E|^2 + \mu_0 |H|^2}{2} \right) \tag{2.85}$$

We now have to calculate the electrical field in the third region. First, we inject Eq. (2.60) in (2.83)

$$\mathbf{E_k} = U_3 \begin{pmatrix} \frac{iq_3 k_x (e^{iq_3(z-h-d)} - e^{2iq_3 L_z} e^{-iq_3(z-h-d)}) \cos(k_x x) \sin(k_y y)}{k_\parallel^2} \\ \frac{iq_3 k_y (e^{iq_3(z-h-d)} - e^{2iq_3 L_z} e^{-iq_3(z-h-d)}) \sin(k_x x) \cos(k_y y)}{k_\parallel^2} \\ (e^{iq_3(z-h-d)} + e^{2iq_3 L_z} e^{-iq_3(z-h-d)}) \sin(k_x x) \sin(k_y y) \end{pmatrix} \tag{2.86}$$

It comes

$$\frac{|\mathbf{E}|^2}{|U_3|^2} = \frac{q_3^2}{k_\parallel^4} |e^{iq_3(z-h-d)} - e^{2iq_3 L_z} e^{-iq_3(z-h-d)}|^2 \left(k_y^2 \sin^2(k_x x) \cos^2(k_y y) \right.$$
$$\left. + k_x^2 \cos^2(k_x x) \sin^2(k_y y) \right) + |e^{iq_3(z-h-d)} + e^{2iq_3 L_z} e^{-iq_3(z-h-d)}|^2 \cos^2(k_x x) \cos^2(k_y y) \tag{2.87}$$

We now derive an expression for $|\mathbf{H}|^2$ in the third region, using the same method.

$$\mathbf{H_k} = \frac{\varepsilon_0 \omega U_3 (e^{iq_3(z-h-d)} + e^{2iq_3 L_z} e^{-iq_3(z-h-d)})}{i k_\parallel^2} \begin{pmatrix} k_y \sin(k_x x) \cos(k_y y) \\ -k_x \cos(k_x x) \sin(k_y y) \\ 0 \end{pmatrix} \tag{2.88}$$

It comes

$$\frac{|\mathbf{H}|^2}{|U_3|^2} = \frac{\varepsilon_0^2\omega^2|e^{iq_3(z-h-d)} + e^{2iq_3L_z}e^{-iq_3(z-h-d)}|^2}{k_\parallel^4}(k_y^2\sin^2(k_xx)\cos^2(k_yy) + k_x^2\cos^2(k_xx)\sin^2(k_yy)) \quad (2.89)$$

Taking a mean value for the terms oscillating with spatial coordiantes, one gets

$$\left\langle \frac{\varepsilon_0|E|^2 + \mu_0|H|^2}{2} \right\rangle_{\mathbf{x}} = \frac{\varepsilon_0^2\mu_0\omega^2|U_3|^2}{2k_\parallel^2} \quad (2.90)$$

We then have

$$W = \frac{V\varepsilon_0^2\mu_0\omega^2|U_3|^2}{2k_\parallel^2} \quad (2.91)$$

We want this energy to be equal to the energy of the vacuum $\frac{\hbar\omega}{2}$. This gives us:

$$\boxed{|U_3|^2 = \frac{\hbar k_\parallel^2}{V\varepsilon_0^2\mu_0\omega}} \quad (2.92)$$

Transition probability induced by the TM modes

We are now in position to compute the transition probability induced by the TM modes. To this end, we compute $|\boldsymbol{\mu}\cdot\mathbf{E}|^2$ in the first region, before using Eq. (1.55). We thus have assumed that the density of modes is identical as the one of the vacuum case.

First, we compute the electrical field in the first region, using Eq. (2.83)

$$\mathbf{E_k} = C_1\begin{pmatrix} \frac{-ik_xq_1\sin(q_1z)\cos(k_xx)\sin(k_yy)}{k_\parallel^2} \\ \frac{-ik_yq_1\sin(q_1z)\sin(k_xx)\cos(k_yy)}{k_\parallel^2} \\ \cos(q_1z)\sin(k_xx)\sin(k_yy) \end{pmatrix} \quad (2.93)$$

Inserting (2.79), it comes

$$\mathbf{E_k} = \frac{2\varepsilon_0(1-r_{23})e^{i(q_1h+q_2d)}(1-r_{12})U_3}{\varepsilon_1\delta}\begin{pmatrix} \frac{-ik_xq_1\sin(q_1z)\cos(k_xx)\sin(k_yy)}{k_\parallel^2} \\ \frac{-ik_yq_1\sin(q_1z)\sin(k_xx)\cos(k_yy)}{k_\parallel^2} \\ \cos(q_1z)\sin(k_xx)\sin(k_yy) \end{pmatrix} \quad (2.94)$$

We now take as convention for the orientation of $\boldsymbol{\mu}$

$$\boldsymbol{\mu} = |\boldsymbol{\mu}|\begin{pmatrix} \sin(\Psi)\cos(\phi) \\ \sin(\Psi)\sin(\phi) \\ \cos(\Psi) \end{pmatrix} \quad (2.95)$$

where Φ and Ψ are Euler angles. We then have:

$$|\mathbf{E_k}\cdot\boldsymbol{\mu}|^2 = \frac{4|\boldsymbol{\mu}|^2|1-r_{12}|^2|1-r_{23}|^2|U_3|^2}{n_1^4|\delta|^2}\Bigg(\left(\frac{q_1^2\sin^2(\Psi)\sin^2(q_1z)}{k_\parallel^4}\right) \times\left(k_x^2\cos^2(k_xx)\sin^2(k_yy)\cos^2(\phi)+k_y^2\sin^2(k_xx)\cos^2(k_yy)\sin^2(\phi)\right) + \cos^2(q_1z)\sin^2(k_xx)\sin^2(k_yy)\cos^2(\Psi)\Bigg) \quad (2.96)$$

Inserting Eq. (2.92)

$$|\mathbf{E_k}\cdot\boldsymbol{\mu}|^2 = \frac{4|\boldsymbol{\mu}|^2|1-r_{12}|^2|1-r_{23}|^2\hbar}{n_1^4V\varepsilon_0^2\mu_0\omega|\delta|^2}\Bigg(\left(\frac{q_1^2\sin^2(\Psi)\sin^2(q_1z)}{k_\parallel^2}\right) \times\left(k_x^2\cos^2(k_xx)\sin^2(k_yy)\cos^2(\phi)+k_y^2\sin^2(k_xx)\cos^2(k_yy)\sin^2(\phi)\right) + k_\parallel^2\cos^2(q_1z)\sin^2(k_xx)\sin^2(k_yy)\cos^2(\Psi)\Bigg) \quad (2.97)$$

We now take an average value on x, y and ϕ

$$\left\langle|\mathbf{E_k}\cdot\boldsymbol{\mu}|^2\right\rangle_{x,y,\phi} = \frac{|\boldsymbol{\mu}|^2|1-r_{12}|^2|1-r_{23}|^2\hbar}{n_1^4V\varepsilon_0^2\mu_0\omega|\delta|^2}\Bigg(\left(\frac{q_1^2\sin^2(\Psi)\sin^2(q_1z)}{2}\right) + k_\parallel^2\cos^2(q_1z)\sin^2(k_xx)\sin^2(k_yy)\cos^2(\Psi)\Bigg) \quad (2.98)$$

Finally, using the desexcitation rule (1.55), one has:

$$P_{i\to f}^{TM} = \frac{|\boldsymbol{\mu}|^2t}{\varepsilon_0\pi\hbar n_1^4}\int_0^k dk_z\frac{|1-r_{12}|^2|1-r_{23}|^2}{|\delta|^2}\Bigg(\frac{q_1^2\sin^2(\Psi)\sin^2(q_1z)}{2} + k_\parallel^2\cos^2(q_1z)\cos^2(\Psi)\Bigg) \quad (2.99)$$

2.2 Transition probability

The sum of both types of electromagnetic modes gives:

$$P_{i\to f} = \frac{|\boldsymbol{\mu}|^2t}{\pi\hbar}\Bigg(\frac{\sin^2(\Psi)\omega^2\mu_0}{2}\int_0^k dk_z\frac{|1-R_{12}|^2|1-R_{23}|^2\sin^2(q_1z)}{|\Delta|^2} + \frac{1}{\varepsilon_0n_1^4}\int_0^k dk_z\frac{|1-r_{12}|^2|1-r_{23}|^2}{|\delta|^2}\left(\frac{q_1^2\sin^2(\Psi)\sin^2(q_1z)}{2}+k_\parallel^2\cos^2(q_1z)\cos^2(\Psi)\right)\Bigg) \quad (2.100)$$

We now use Eq. (1.73) to normalise this result

$$P_{i\to f} = 3\Gamma_1 t \left(\frac{\sin^2(\Psi)}{2\omega\sqrt{\mu_0\varepsilon_1}} \int_0^k dk_z \frac{|1-R_{12}|^2|1-R_{23}|^2\sin^2(q_1 z)}{|\Delta|^2} \right.$$
$$\left. + \frac{1}{n_1^4\omega^3\mu_0^{3/2}\varepsilon_0\sqrt{\varepsilon_1}} \int_0^k dk_z \frac{|1-r_{12}|^2|1-r_{23}|^2}{|\delta|^2} \left(\frac{q_1^2\sin^2(q_1 z)}{2}\sin^2(\Psi) + k_\parallel^2\cos^2(q_1 z)\cos^2(\Psi) \right) \right) \tag{2.101}$$

Equivalently, with $k = \frac{\omega}{c}$:

$$P_{i\to f} = 3\Gamma_1 t \left(\frac{\sin^2(\Psi)}{2n_1 k} \int_0^k dk_z \frac{|1-R_{12}|^2|1-R_{23}|^2\sin^2(q_1 z)}{|\Delta|^2} \right.$$
$$\left. + \frac{1}{n_1^5 k^3} \int_0^k dk_z \frac{|1-r_{12}|^2|1-r_{23}|^2}{|\delta|^2} \left(\frac{q_1^2\sin^2(q_1 z)\sin^2(\Psi)}{2} + k_\parallel^2\cos^2(q_1 z)\cos^2(\Psi) \right) \right) \tag{2.102}$$

We now define the relative transition rate as

$$\Gamma_r = \frac{P_{i\to f}}{\Gamma_1 t} \tag{2.103}$$

Two particular cases can be expressed:

- $\Gamma_\perp$, expressing the desexcitation rate of an exciton whose dipole is oriented in the direction z. In this case, $\Psi = 0$
- $\Gamma_\parallel$, expressing the desexcitation rate of an exciton whose dipole is transverse to the plane (x, y). In this case, $\Psi = \pi/2$

Thus,

$$\Gamma_\perp = \frac{3}{n_1^5 k^3} \int_0^k dk_z \frac{|1-r_{12}|^2|1-r_{23}|^2}{|\delta|^2} k_\parallel^2\cos^2(q_1 z) \tag{2.104}$$

$$\Gamma_\parallel = \frac{3}{2n_1 k} \left(\int_0^k dk_z \frac{|1-R_{12}|^2|1-R_{23}|^2\sin^2(q_1 z)}{|\Delta|^2} \right.$$
$$\left. + \frac{1}{n_1^4 k^2} \int_0^k dk_z \frac{|1-r_{12}|^2|1-r_{23}|^2 q_1^2\sin^2(q_1 z)}{|\delta|^2} \right) \tag{2.105}$$

Another important result can be expressed by taking a mean value along the possible orientations of the dipole for the desexcitation rate. As directions

x and y correspond to $\Psi = \pi/2$ and direction z corresponds to $\Psi = 0$, the mean desexcitation rate can be expressed as

$$\Gamma_r = \frac{\Gamma_\perp}{3} + \frac{2\Gamma_\parallel}{3}. \tag{2.106}$$

Injecting Eqs. (2.104) and (2.105) in Eq. (2.106), it comes

$$\begin{aligned}\Gamma_r = \frac{1}{n_1 k}\Bigg[&\int_0^k dk_z \frac{|1-R_{12}|^2|1-R_{23}|^2\sin^2(q_1 z)}{|\Delta|^2} \\ &+\frac{1}{n_1^4 k^2}\int_0^k dk_z \frac{|1-r_{12}|^2|1-r_{23}|^2}{|\delta|^2}\left(q_1^2\sin^2(q_1 z)+k_\parallel^2\cos^2(q_1 z)\right)\Bigg]\end{aligned} \tag{2.107}$$

Chapter 3

Numerical simulations

In this chapter, we set a range of the parameters of the solar cell, before computing equations (2.107), (2.105) and (2.104).

3.1 Parameters range

We used for the refractive index of region 2 the one of the Gallium doped Zinc oxide, a conducting, optically transparent material, suitable for PV technology [22]. Its value is [24] :

$$n_2 = 2. \tag{3.1}$$

The wavevector and real refractive index of the polymer are taken from [11], supposing a zero extinction coefficient

$$n_1 = 1.6 \qquad k = \frac{2\pi}{600\text{nm}} = \frac{\pi}{300}\text{nm}^{-1} \tag{3.2}$$

The parameters h and d can then be optimised around their typical values: those of thin film solar cells

$$h \approx 100\text{nm} \qquad d \approx 5\text{nm} \tag{3.3}$$

3.2 Simulations

3.2.1 Reference case

We plotted the equations (2.107), (2.105) and (2.104) using Mathematica 7.0, for the reference case, chosen to have $h = 100$nm and $d = 5$nm. Fig. 3.2 represents the mean decay probability as a function of the position in the

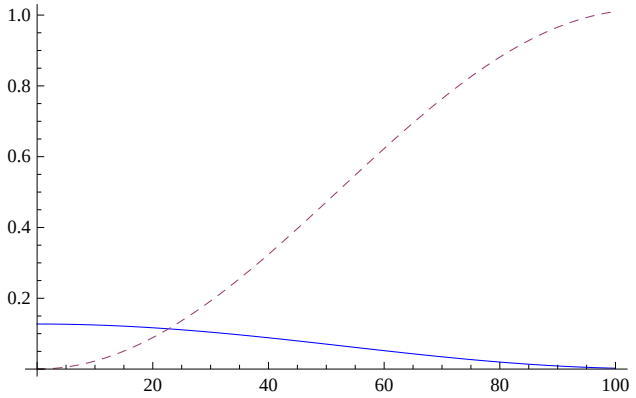

Figure 3.1: Decay probability as a function of the position in nanometers in the active region for the parameters: $n_1 = 1.6$, $n_2 = 2$, $h = 100$nm, $d = 5$nm, $k = \frac{\pi}{300}\text{nm}^{-1}$. Full line: $\Psi = 0$. Dashed line: $\Psi = \pi/2$

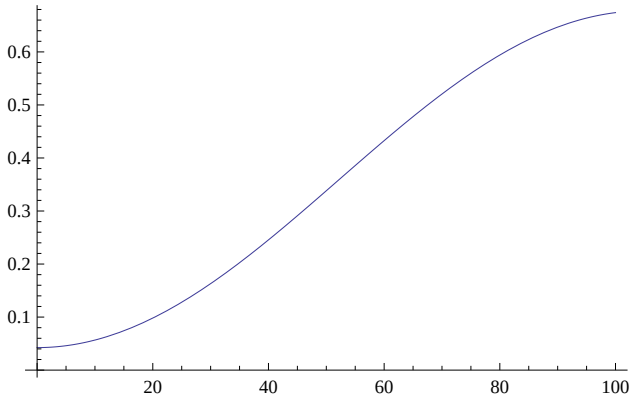

Figure 3.2: Mean decay probability (Eq. (2.107)) as a function of the position in nanometers in the active region for the parameters: $n_1 = 1.6$, $n_2 = 2$, $h = 100$nm, $d = 5$nm, $k = \frac{\pi}{300}\text{nm}^{-1}$

active region (Eq. (2.107)). In Fig. 3.1 the desexcitation rate is splitted in its two components, which are described by the equations (2.104) and (2.105).

In Fig. (3.1), one notices that $\Gamma_\perp$ is much smaller than $\Gamma_\parallel$ in the biggest part of the active region.

3.2.2 Modification of the active region length

To begin with, we made the distance h smaller. We chose its value to be 30nm. Fig 3.4 shows the mean spontaneous emission rate, whereas Fig. 3.3 displays Eqs. (2.104) and (2.105) for the same parameters.

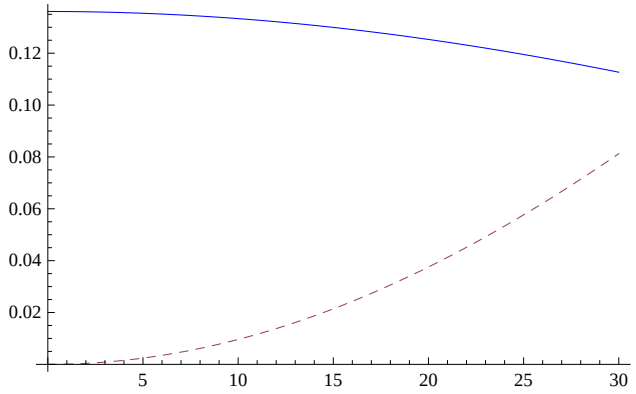

Figure 3.3: Decay probability as a function of the position in nanometers in the active region for the parameters: $n_1 = 1.6$, $n_2 = 2$, $h = 30$nm, $d = 5$nm, $k = \frac{\pi}{300}\text{nm}^{-1}$. Full line: $\Psi = 0$. Dashed line: $\Psi = \pi/2$

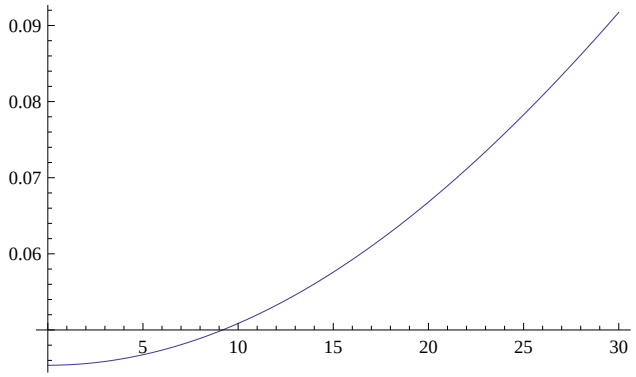

Figure 3.4: Mean decay probability (Eq. (2.107)) as a function of the position in nanometers in the active region for the parameters: $n_1 = 1.6$, $n_2 = 2$, $h = 30$nm, $d = 5$nm, $k = \frac{\pi}{300}\text{nm}^{-1}$

To compare those results, we have chosen to plot many curves for h varying from 30 to 100 nanometers. This is shown Fig. 3.5, for the 30 nanometers closest to the collecting electrode.

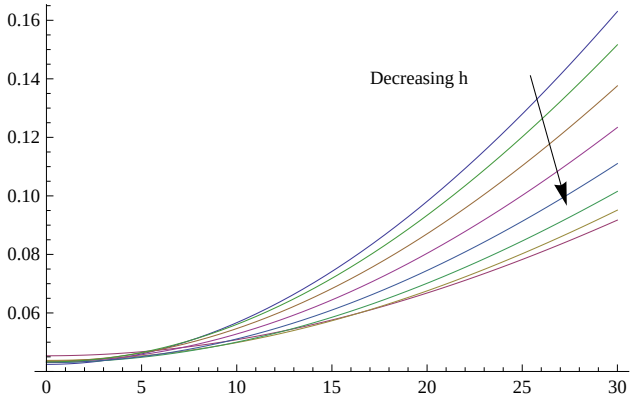

Figure 3.5: Mean decay rate as a function of z, for different values of h, between 30 and 100nm. All other parameters identical to those of Fig. 3.2

This reduction has a small but visible effect on the desexcitation close to the collecting electrode: the thinner the active region, the smaller the desexcitation rate. A compromise has then to be made between the generation of excitons, varying as the thickness does, and the desexcitation of those excitons. However, the "thin" geometry is often prefered because of the diffusion length of the excitons: the excitons are created near the electrode, so that they immediately can recombine.

3.2.3 Modification of the semitransparent electrode thickness

We now make the semitransparent electrode thicker: we chosen its value to be $d = 20$nm. In Fig. 3.7 stands a plot of Eq. (2.107), in Fig. 3.1 stand plots of Eqs. (2.105) and (2.104).

As we did for the reduction of the length of the active region, we compared the mean desexcitation rate for different values of d. In this case, we chose to make d change from 2 to 25 nm. This is plotted in Fig. 3.8.

One remarks that effects of reducting the electrode thickness are not as surprising as the active region reduction effects were. However, we also remark that the thicker the electrode the larger the desexcitation rate. In practice, the electrode has to be thick enough to provide conductivity[22].

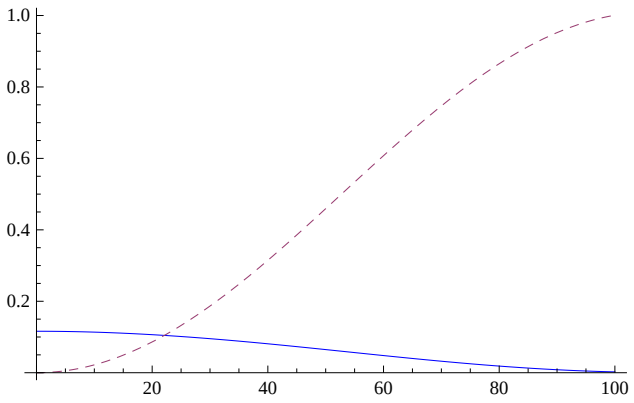

Figure 3.6: Decay probability as a function of the position in nanometers in the active region for the parameters: $n_1 = 1.6$, $n_2 = 2$, $h = 100\text{nm}$, $d = 20\text{nm}$, $k = \frac{\pi}{300}\text{nm}^{-1}$. Full line: $\Psi = 0$. Dashed line: $\Psi = \pi/2$

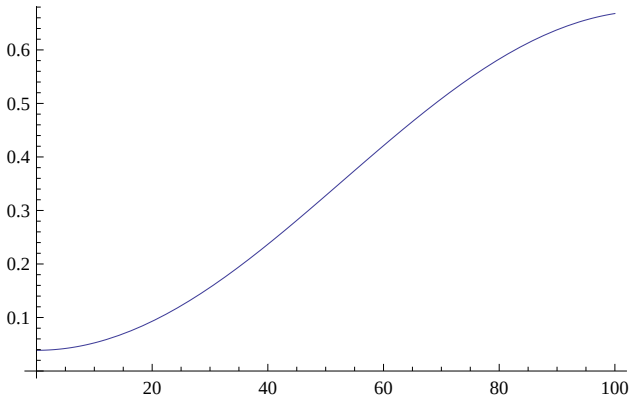

Figure 3.7: Mean decay probability (Eq. (2.107)) as a function of the position in nanometers in the active region for the parameters: $n_1 = 1.6$, $n_2 = 2$, $h = 100\text{nm}$, $d = 20\text{nm}$, $k = \frac{\pi}{300}\text{nm}^{-1}$

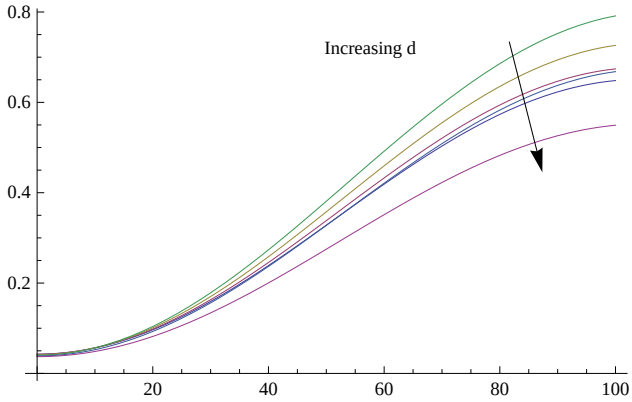

Figure 3.8: Mean decay rate as a function of z, for different values of d, between 2 and 25nm. All other parameters identical to those of Fig. 3.2.

Chapter 4

Discussion

In this chapter, we discuss the equations (2.36) and (2.81), before proposing ways to improve PV devices.

4.1 Characteristic equations 2.36 and 2.81

In this section, we discuss the characteristic equations (2.36) and (2.81). Those equations can be regarded as equations describing the possible states of the system. This is an important part of the treatment, which has actually not been done in the preceeding sections. Eqs. (2.36) and (2.81) can be rewritten as

$$\Delta e^{2iq_3L_z} - R_{23}e^{2i(q_1h+q_2d)} - R_{23}R_{12}e^{2iq_2d} - e^{2iq_1h}R_{12} - 1 = 0, \tag{4.1}$$

$$\delta e^{2iq_3L_z} + r_{23}e^{2i(q_1h+q_2d)} - r_{12}r_{23}e^{2iq_2d} + r_{12}e^{2iq_1h} - 1 = 0. \tag{4.2}$$

One can then plot the modulus of the left hand side of each equation versus the wavenumber k_z, varying between 0 and k, for different values of L_z. Figure 4.1 displays this method applied to Eq. (4.1), and Fig. 4.2 displays this method applied to Eq. (4.2).

As the possible states of the system are the solutions of the characteristic equations, they correspond in Figs. 4.1 and 4.2 to intersections of the curves with the abscis axis. For the sake of readability, only two values for L_z have been taken into account in those figures, but other simulations tend to confirm the depicted inclination: the bigger L_z, the more solutions to Eqs. (4.1) and (4.2) there is.

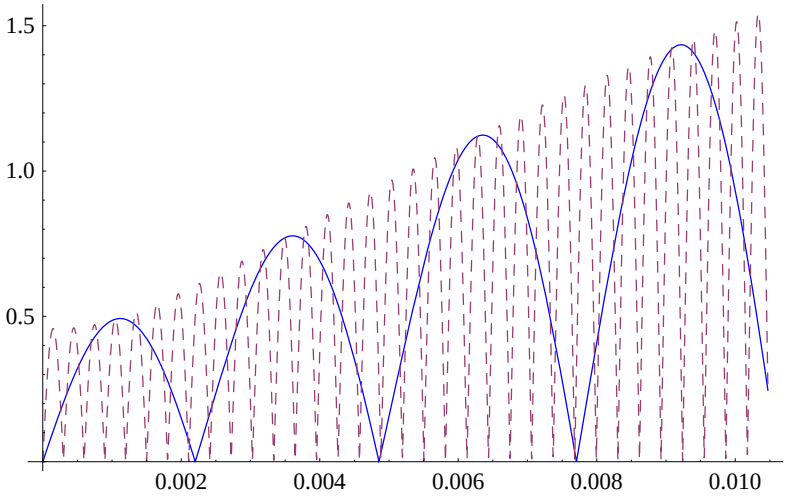

Figure 4.1: $|\Delta e^{2iq_3L_z} - R_{23}e^{2i(q_1h+q_2d)} - R_{23}R_{12}e^{2iq_2d} - e^{2iq_1h}R_{12} - 1|$ versus k_z. Full: $L_z = 1000$. Dashed: $L_z = 10000$

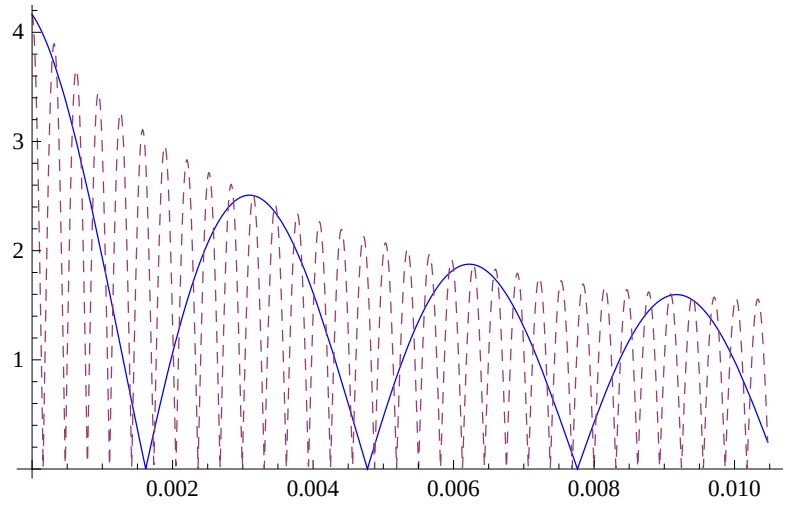

Figure 4.2: $|\delta e^{2iq_3L_z} + r_{23}e^{2i(q_1h+q_2d)} - r_{12}r_{23}e^{2iq_2d} + r_{12}e^{2iq_1h} - 1|$ versus k_z. Full: $L_z = 1000$. Dashed: $L_z = 10000$

By choosing the approach developped in this work, we thus assumed that:

- As L_z tends to infinity, the number of solution of Eqs. of the variable k_z (4.1) and (4.2) does so and
- The density of solutions in k_z is in this case uniform in the interval $[0, k]$.

Numerical simulations tend to confirm those assumptions.

4.2 Ways to improve PV devices

The results of the work done here will be useable as soon as a reliable photovoltaic polymer presenting a high quantum yield is available. When its parameters will be known, this model will allow a computation of the desexcitation rate in the solar cell. The approach developped in this work is also applied to a particularly simple Fabry-Pérot type geometry: it surely can be interesting to extand the treatment we made to some other structures.

Conclusion

In order to enhance PV cell conversion efficiency, we presented in this work a theoretical model based on Fermi Golden Rule to compute the spontaneous emission rate in a PV cell as a function of its dielectric and geometric parameters.

We modelled an exciton as the upper energy state of a two-level system to first make the two-level system evolve in vacuum. Then, we perturbed this system by adding an interaction with an electromagnetic field. This electromagnetic field was further described as the vacuum fluctuations of a cavity. Therewith, we derived an evolution law in vacuum, before extending it to an homogeneous dielectric medium.

We then modelled a PV cell as a superposition of three dielectric media, containing a two-level system in its excited state in the first of those. We then derived an evolution law for this system, following the approach we followed in the vacuum case.

Although the results we presented were not coupled to the diffusion equation (1.5) and/or current equations, they are quite encouraging. Indeed, the spontaneous emission rate can, in some cases (see e.g. Fig. 3.4) be reduced to 10% of the free space value.

However, a reduction of 90% of spontaneous emission rate induces, for a polymer presenting a quantum yield close to 1, "only" an increase of diffusion length up to

$$L = \sqrt{\frac{D}{\Gamma_r \Gamma_1}} = \frac{1}{\sqrt{\Gamma_r}} \sqrt{\frac{D}{\Gamma_1}}. \tag{4.3}$$

By denoting L_1 the diffusion length in an homogeneous dielectric medium of permittivity ε_1, one has

$$L = \frac{L_1}{\sqrt{\Gamma_r}} \approx 3.16 L_1 \tag{4.4}$$

So an enlegthment is not as impressive as the "90% reduction in spontaneous emission" are, but it is a great advance.

However, the model we developed still has to be checked, experimentally and theoretically. From an experimental point of view, this work can also be seen as a motivation for chemists to develop a high quantum yield PV polymer.

From a theoretical point of view, this model can be developed by e.g. considering a finite bandwidth for the exciton desexcitation, defining a quality factor of the PV cell such as an optimisation of the dielectric and geometrical parameters would be mathematically determinable, extending this method to other geometries, taking into account the imaginary part of refractive indexes...

This model can also be checked, using a fully quantised model, or simplified, using classical electrodynamics theory.

Bibliography

[1] "International Energy Outlook",Doman, E.Linda et al., EIA,2009

[2] "Thin Film Solar Cells", A.G. Aberle, Thin Solid Films 517, 2009

[3] "Polymer-based solar cells"A.C. Mayer et al., materialstoday, 2007

[4] http://en.wikipedia.org/wiki/File:PVeff%28rev100414%29.png

[5] http://upload.wikimedia.org/wikipedia/commons/b/b4/Silicon_covalent_bond.PNG

[6] "Optoelectronics of solar cells", G.P. Smestad, SPIE, 2002

[7] "Introduction to Solid State Physics " 4th edition, C. Kittel, John Wiley & sons, 1971

[8] "Science and technology of photovoltaics" 2nd Edition, P. Jayarama Reddy, CRC Press, 2010

[9] http://upload.wikimedia.org/wikipedia/commons/f/fa/Pn-junction-equilibrium-graphs.png

[10] http://upload.wikimedia.org/wikipedia/commons/4/46/Bandgap_in_semiconductor.svg

[11] "Cavity-controlled radiative recombination of excitons in thin-film solar cells", L.T. Vuong et al., Applied Physics Letters 95,2009

[12] "Merocyanine organic solar cells" A.K. Ghosh & T. Feng, J. Appl. Phys . 49, 1978

[13] "Light trapping properties of pyramidally textured surfaces" P. Campbell et al., J.Appl.Phys. 62,1987

[14] "High voltage vertical multijunction solar cell", R.J. Soukup, J.Appl. Phys 47, 1976

[15] "Practical antireflexion coatings for metal semiconductor solar cells" , Y.C.M.Yeh et al. J. Appl. Phys 47, 1976

[16] "Theory of metal-insulator-semiconductor solar cells",J. Swewchun et al . J.Appl.Phys. 48,1977

[17] "PV solar cells: New challenge for chemical physics",O.Shevaleevskiy, Pure Appl. Chem.,2008

[18] "Lasers et Optique non linéaire", C. Delsart, Ellipses, 2008

[19] "Mécanique quantique",C. Cohen Tannoudji et al., Hermann,1973

[20] `http://upload.wikimedia.org/wikipedia/commons/0/02/Cube.svg`

[21] "Light Volume 1: Waves, Photons, Atoms", H Haken, North Holland, 1981

[22] "Zinc oxide, a multifunctional material: from material to device applications", E. Fortunato et al., Applied Physics A 96, 2009

[23] "Classical Electrodynamics" 2nd Edition, J.D Jackson, J. Wiley & Sons, 1975

[24] "High quality conductive gallium-doped zinc oxide films deposited at room temperature", E. Fortunato et al., Thin Solid Films 451-452, 2004